DOI: 10.1002/cbic.200900277

Spatio-Temporal Control of Cell Coculture Interactions on Surfaces

Eun-Ju Lee, Eugene W. L. Chan, and Muhammad N. Yousaf*[a]

Mammalian tissues are composed of various cell types that interact with each other in a constantly changing dynamic microenvironment.[1–5] Cell behavior and function is determined by a range of factors including soluble signals from cells of the same type (autocrine signaling), as well as those from other cell types (paracrine signaling),[6,7] and physical-mechanical and hydrodynamic forces.[8–10] There have been numerous reports showing the critical role that cell–cell interactions play in modulating overall cellular or tissue function from cell growth, migration, and differentiation to embryonic development.[11–15] For example, heterotypic cell interactions between parenchymal cells and nonparenchymal neighbors alter cell growth, migration, and differentiation.[12] In cocultures of transgenic cells and wild type cells, the release of regulatory signals by wild type cells helps the transgenic cells restore their cellular function.[16] Furthermore, lineage commitment of mesenchymal progenitor cells is directly influenced by cell signaling from adjacent cells.[17]

To study these complex events there have been several approaches to develop spatially controlled micropatterned coculture model systems to mimic inter- and intracellular interactions. These strategies include thermo-responsive polymer surfaces,[18,19] soft-lithography-generated substrates[20–22] and patterned extracellular matrix (ECM) surfaces.[23] For temporal control of cell culture, dynamic surfaces have been generated, and for cocultures a micromechanical strategy has been employed.[24] Although there has been significant progress in developing patterned cell surfaces, there are no coculture model substrates that are able to: 1) Reversibly control the interactions between different cell populations that are in patterns on molecularly defined surfaces and 2) Serially manipulate the surface to control the duration of the cell interactions. These features would allow for many new studies of cell–cell interactions for a range of cell biological and physiological research fields.

Herein we report a combined photochemical and electroactive self-assembled monolayer (SAM)-based substrate strategy to generate a coculture platform with spatial and temporal control of cell–cell interactions. These substrates possess the ability to present a variety of ligands on the surface for biospecific interactions between the immobilized ligands and cell surface receptors. Furthermore, the photopatterning step enables the ligands to be immobilized in complex patterns and even gradients. This feature provides additional flexibility to study the role of ligand pattern (geometry) and presentation on coculture interactions on complex surfaces.

The general surface chemistry strategy to pattern, immobilize, and release ligands is shown in Scheme 1. A hydroquinone alkanethiol (**1**) that has been protected with a photolabile group (nitroveratryloxycarbonyl or NVOC) is installed onto a surface and then deprotected by using ultraviolet light ($h\nu$) to generate the hydroquinone (H_2Q, **2**).[25] The hydroquinone is redox active and can be converted to the quinone (Q) through a mild electrochemical oxidation for subsequent immobilization of oxyamine tethered ligands (R-ONH_2).[26,27] The interfacial oxime conjugate is also redox active and can be made to release the ligand through a mild reductive potential; this regenerates the hydroquinone.[28] The immobilization and release of ligands is compatible with adhered cells and cell culture conditions, and has no side reactions or adverse effects to the cells.[26,28]

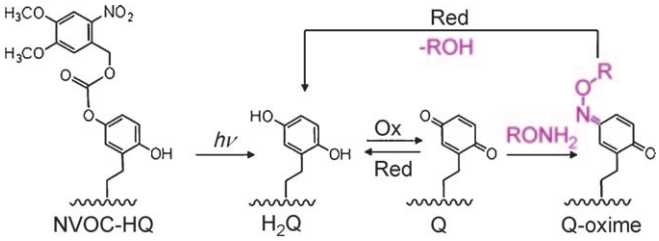

Scheme 1. Surfaces presenting NVOC-protected hydroquinone groups (NVOC-HQ) are illuminated with ultraviolet light (365 nm). Photochemical deprotection of the NVOC group reveals the hydroquinone (H_2Q). Subsequent oxidation of the hydroquinone results in the corresponding quinone (Q), which can then undergo chemoselective ligation with aminooxy terminated ligands ($RONH_2$) to generate a stable and covalent oxime conjugate (Q-oxime). The oxime is also redox active and can be reduced to regenerate the hydroquinone with the simultaneous release of ligand through a mild reductive electrochemical potential at pH 7.4. R represents rhodamine, and the cell adhesive peptide GRGDS.

For spatial and temporal control of coculture interactions we combined the photoelectroactive surface chemistry strategy with a microcontact printing (μCP) patterning method (Scheme 2).[25,29] We first used μCP to selectively pattern hexadecanethiols (HDTs) onto a gold surface to generate hydrophobic regions. The remaining bare gold regions were backfilled with a mixed solution of tetra(ethylene glycol)-terminated alkanethiols (EG_4SH, **3**) and NVOC-protected hydroquinone-terminated alkanethiols (**1**) (99:1 ratio). The use of a high percentage of tetra(ethylene glycol)-terminated alkanethiols renders the nonpatterned regions inert to nonspecific protein or cell attachment.[30] Ultraviolet light was shone on this SAM surface through a patterned photomask to selectively deprotect the NVOC groups to hydroquinone groups. To facilitate cell adhe-

[a] E.-J. Lee, Dr. E. W. L. Chan, Prof. M. N. Yousaf
Department of Chemistry and the Carolina Center for Genome Sciences
University of North Carolina at Chapel Hill
Chapel Hill, North Carolina 27599-3290 (USA)
Fax: (+1) 919-962-2388
E-mail: mnyousaf@email.unc.edu

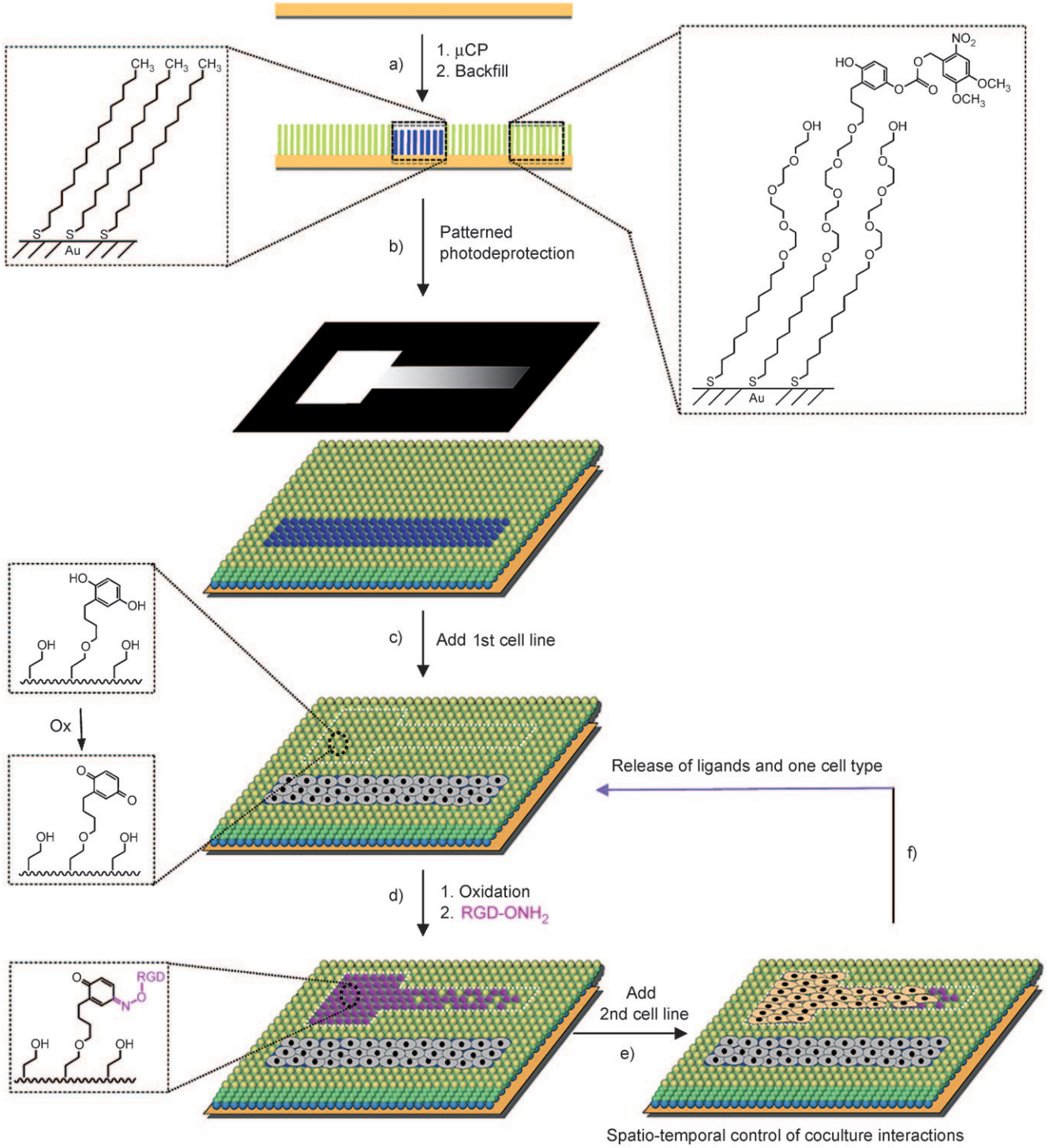

Scheme 2. Schematic diagram of substrate preparation for dynamic coculture substrates. A glass coverslip was coated with Ti (3 nm) and then gold (12 nm) by an electron-beam deposition method. A) To generate patterned surfaces, hexadecanethiols were microcontact printed onto the gold surface and the remaining bare gold regions were backfilled with a mixture of NVOC-HQ and EG_4SH (1:99 ratio). B) The substrate was illuminated with UV light through a patterned microfiche mask; this resulted in the selective deprotection of NVOC groups to reveal the electroactive hydroquinone. C) An adhesive protein, fibronectin, was added to the substrate and only adsorbed to the hydrophobic microcontact-printed pattern. Cells were seeded onto the entire substrate but exclusively adhered to the fibronectin-patterend regions. D) The patterned hydroquinone groups were then converted to reactive quinone groups through application of a mild oxidative electrochemical potential. Addition of soluble RGD-ONH_2 led to the installation of the adhesive peptide to the patterned quinone region through the formation of a stable covalent oxime linkage. E) Addition of a second cell line generated patterned cocultures with exquisite spatial control. F) After a period of time, application of a mild reductive electrochemical potential causes breakage of the oxime linkage and release of RGD peptides; this in turn causes one population of cells to release from the surface. This strategy allows for the analysis of both cell types through spatial and temporal control of their interactions on a surface.

sion to the microcontact printed regions, a fibronectin solution (10 mM in PBS, 1 h) was added to the entire surface, but exclusively adsorbed to the hydrophobic pattern.[31] The first fibroblast cell type was then seeded onto the surface and selectively adhered and stayed confined to the fibronectin/microcontact-printed regions. The hydroquinone groups in the photopatterned area were then electrochemically oxidized to quinones. This oxidation is mild and rapid and is compatible with cell culture conditions. The electroactive substrate allows for the precise monitoring of the immobilization and release of ligands to and from the surface by cyclic voltammetry.[26,27] Soluble oxyamine-RGD (**4**) (50 mM, 1 h in PBS pH 7.4) was added, and this installed the adhesive peptide onto the photopatterned area through the formation of an oxime linkage to the quinone. Addition of the oxyamine-RGD allowed for the adherence of a second cell type in a distinct pattern on the surface. The RGD peptide ligand is derived from the extracellular matrix protein fibronectin and is known to facilitate biospecific cell adhesion through cell-surface integrin receptors.[32] This coupling reaction is chemoselective and fast and can be carried out in the presence of the first cell type pattern without loss of cell function or pattern.[26] When a second cell type was added, the cells selectively adhered only to the photopatterned RGD region. For temporal control, the second cell type can be released from the pattern by a simple application of a mild reductive electrochemical potential (−50 mV, 1 min in serum-free medium, pH 7.4). The oxime linkage is broken and the RGD ligand is released from the surface while the hydroquinone is regenerated. The second cell type then loses its attachment to the support and therefore is released from the surface. This methodology is able to spatially and temporally control cell–cell interactions on a molecularly defined surface in various patterns and has the ability to immobilize and release a range of ligands (**1**–**5**) and cell types.

The photopatterning method provides an important feature in that ligand molecules can be installed onto the surface in virtually any geometric pattern and even complex patterns such as gradients. By employing a photomask with a patterned gradient design, a ligand gradient with control of pattern and slope can be generated on the surface; this can elicit a complex cellular response within the pattern on a coculture surface. This particular flexibility allows complex cell–cell signaling to be examined. Also, the role of patterned cocultures on cell behavior can be studied in cases which each cell type patterned might be undergoing discrete processes such as migration, growth, or differentiation, depending on the underlying surface chemistry composition.[33,34]

The characterization of a gradient surface generated by the photopatterning strategy is shown in Figure 1. Fluorescence microscopy was used to visualize a rhodamine-oxyamine (**5**) immobilized gradient pattern.[25,26] The slope was determined from the fluorescent gradient pattern by using imaging software and was in accord with the corresponding gradient slope of the photomask. When the same procedure was used but instead a RGD-oxyamine peptide was immobilized, seeded cells first attached to the high density region of the gradient. The cells then migrated and proliferated down the gradient until the ligand density no longer supported migration or division. The cells achieved this equilibrium or final resting position on the gradient after approximately three days. Figure 1C shows a plot for the relative density with respect to the distance along the gradient generated from ImageJ software. To extrapolate the density along the gradient from this plot, we assume that the maximum peptide density is 2.7×10^4 molecules per μm^2 based on a 1% NVOC hydroquinone monolayer that has been completely modified to the peptide ligand on the surface. The ligand density at 1% NVOC hydroquinone was determined based on integration of the area under the oxidative or reductive waves corresponding to the hydroquinone monolayer after the photodeprotection of monolayer presenting only the NVOC hydroquinone groups. By aligning the density plot with the patterned cells (averaged over twelve experiments), we can determine the minimum ligand density for supporting cell adhesion along this particular gradient (ca. $0.16\% = 0.43\times10^4$ molecules per μm^2).

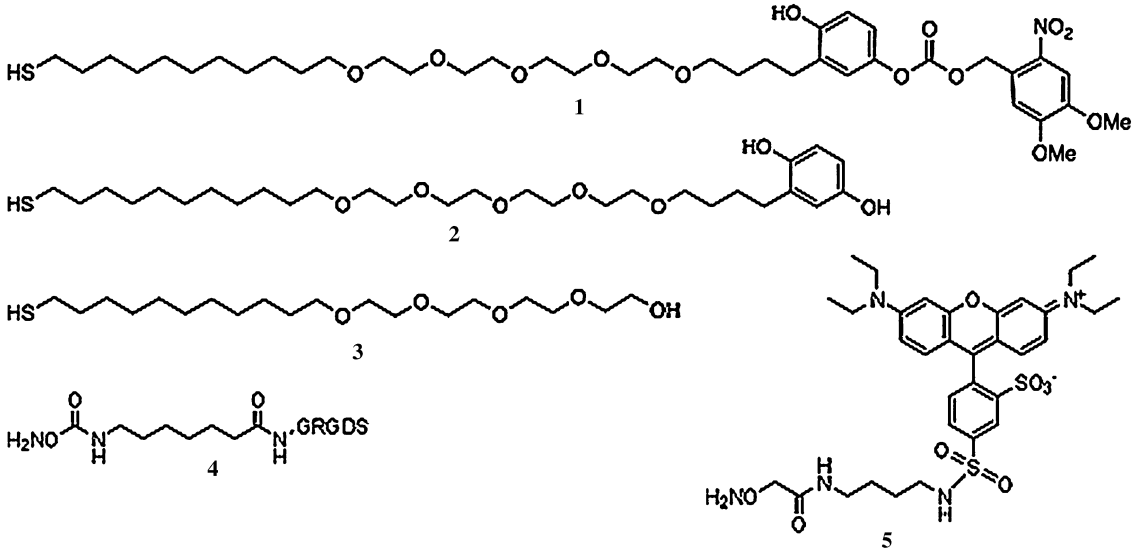

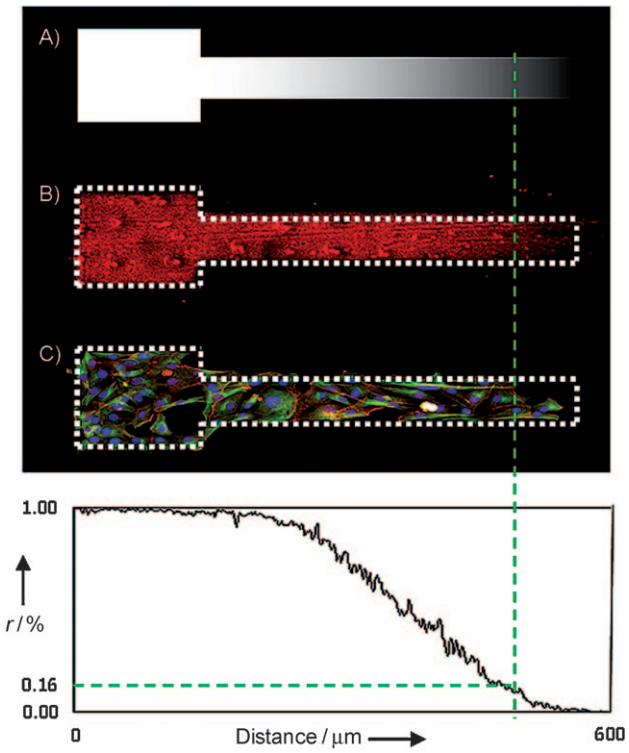

Figure 1. Characterization of a ligand gradient on a surface generated by photopatterning and subsequent electroactive ligand immobilization. A) A microfiche mask with gradient pattern. B) The fluorescent micrograph shows the fidelity of surface patterning. First, UV illumination through the mask was performed, and then electroactive conversion from the hydroquinone to the quinone was carried out; this was followed by rhodamine-oxyamine immobilization to generate the oxime conjugate. Imaging software was used to calculate the gradient slope from the fluorescent image and corresponds to the microfiche mask gradient. C) In parallel experiments RGD-ONH_2 was immobilized to the photodeprotected pattern to which cells biospecifically adhered through their integrin receptors (colors; red, actin; green, tubulin; blue, nuclei). By comparing the position of the cells at the lowest end of the gradient with the slope profile generated from the fluorescent gradient, the minimum required ligand density (Γ) for cell adhesion can be determined. In this example, cell adhesion was greatly diminished when the ligand density was reduced to 0.16% from the highest ligand density used (see text for details).

We observed that the slope of the gradient influences the final position of the cells and found that the steeper the slope, the higher the ligand density required to support adhesion. Conversely, the shallower the slope, the lower the ligand density required to support adhesion. Interestingly, our data show that the minimum ligand density varies on each gradient. Therefore, the cells are able to sense the slope and alter their position based on the combination of slope and ligand density. We are exploring how the spatial distribution (front to back) of cellular focal adhesions, which connect the integrin receptors to the extracellular RGD ligands, transduces the slope and density information to the actin cytoskeleton and induces cell polarity and directed cell migration.[25,35] This strategy allows for the immobilization of a variety of ligands to a patterned gradient surface to study a range of cellular behavior.

To demonstrate a dynamic coculture in which two cell lines can be patterned in close proximity with different underlying surface chemistries, we combined μCP with our electroactive immobilization and release strategy. Figure 2 shows micrographs of two different patterned cell lines. The microcontact printed area (rectangular shape) contains a stably transfected mouse fibroblast cell line expressing GFP-actin.[36] The photopatterned RGD region contains a nonfluorescent mouse fibroblast cell line. The spatial interactions between cocultures can be precisely controlled by varying the pattern size, geometry and distance of the two patterns by employing soft lithography and photomasks. Temporal control over the coculture interactions can be regulated by electrochemistry. After the two cell types are patterned, one cell type can be selectively released by the application of a mild electrochemical potential; this releases the RGD ligands and therefore one of the patterned cell types. This method allows for spatial and temporal control of coculture interactions on surfaces that can be tailored with a variety of ligands. Furthermore, thy ways in which a ligand gradient influences cellular behavior and coculture communication can also be explored.

In summary, we have generated a dynamic substrate with spatial and temporal control of coculture interactions. This strategy relies on a photopatterning and electroactive immobilization and release strategy in combination with μCP. This strategy is flexible in that ligands can be presented on the surface in complex patterns and gradients to study the interplay of ligand density, ligand affinity, pattern geometry, ligand slope and distance between cocultures for a range of autocrine and paracrine signaling studies. As a biotechnology platform, this system may also allow for the modular patterning and exchange of multiple cell lines to a single surface for novel small molecule and RNAi coculture screens.[37]

Experimental Section

Synthesis of alkanethiolates: NVOC-protected hydroquinone tetra(ethylene glycol) alkanethiol, tetra(ethylene glycol) alkanethiol, and rhodamine oxyamine were prepared as previously described.[25,26]

Solid-phase peptide synthesis: All peptides were synthesized through automated solid phase peptide synthesis by using the CS136XT Peptide Synthesizer (CS Bio Co., Menlo Park, CA, USA).

RGD-oxyamine (4): Fmoc (9-fluorenylmethoxycarbonyl)-protected amino acids were used on Fmoc-Ser(*t*Bu)-Rink Amide-MBHA resin. The synthesized peptide was cleaved from the resin by agitation in a solution of trifluoroacetic acid (TFA)/water/triisopropylsilane (95:2.5:2.5) for 3 h. TFA was evaporated and the cleaved peptide was precipitated in cold diethyl ether. The water-soluble peptide was extracted with water and lyophilized. Mass spectral data confirmed the peptide product. MS (ESI) (*m/z*): [M+H^+] calculated for linear RGD-oxyamine ($C_{25}H_{45}N_{11}O_{11}$), 676.69; found, 676.5. [M+H^+] calculated for control scrambled peptide, GRD-oxyamine ($C_{25}H_{45}N_{11}O_{11}$), 676.69; found, 676.4. [M+H^+] calculated for control soluble peptide RGD ($C_{17}H_{31}N_9O_8$), 490.48; found, 490.3.

Microscopy of surface immobilized rhodamine: Scotch tape (3M, Minneapolis, MN, USA) was adhered to the monolayer. The resulting substrate was then cured at 85 °C for 20 min. The tape was

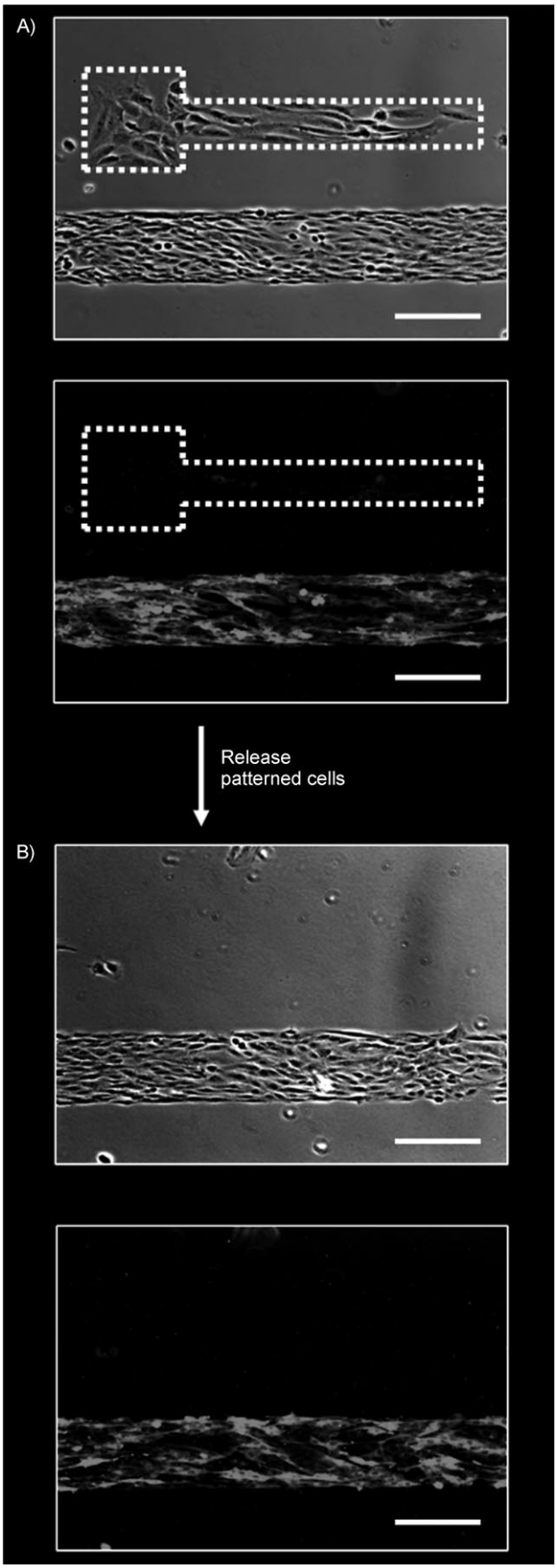

peeled from the substrate; this resulted in the transfer of the monolayer from the gold substrate to the tape. The resulting image was quantified by using fluorescent microscopy and Image J software.

Microscopy of attached cell culture: Adherent cells were fixed in paraformaldehyde (3.7%) in phosphate buffered saline (PBS) for ten minutes and then permeabilized with Triton X (0.1%) in PBS (PBST) for ten minutes. Cells were then stained with anti-tubulin (1:1000) in PBS that contained goat serum (10%) for one hour, followed by staining with an Alexa 488-conjugated goat anti-mouse antibody (1:100 in PBST), phalloidin-tetramethylrhodamine B isothiocyanate (1:50 in PBST), and DAPI (1:300 in PBST) for one hour. Substrates were rinsed with deionized water before being mounted onto glass cover slips for microscopy. All optical and fluorescent micrographs were imaged using a Nikon inverted microscope (model TE2000-E). All images were captured and processed by MetaMorph.

Preparation of monolayers: All gold substrates were prepared by electron-beam deposition of titanium (3 nm) and then gold (12 nm) on glass cover slips (75 mm x 25 mm). All gold-coated glass substrates were cut into 1 cm^2 pieces and washed with absolute ethanol. The substrates were immersed in an ethanolic solution containing the alkanethiolates (1 mM) for 12 h, and then cleaned with ethanol prior to each experiment.

Electrochemical measurements in cell culture: All electrochemical experiments were performed by using a Bioanalytical Systems CV-100W potentiostat (West Lafayette, USA). For RGD peptide immobilization, electrochemical oxidation of the monolayer was performed by applying an oxidative potential at 750 mV for 10 s in PBS (pH 7.4). Addition of 50 mM RGD-ONH_2 installed the peptide onto the surface. For RGD peptide release from the surface, a reductive potential of −50 mV was applied for 1 min in serum free media (pH 7.4). A platinum wire was used as the counter electrode, Ag/AgCl was used as a reference, and the gold/SAM substrate was used as the working electrode.

Fabrication of photomasks: The photopatterns were designed and drawn in PowerPoint. The patterns were then reduced 25 times and printed onto microfiches.

Photochemical deprotection of substrates: A substrate presenting NVOC-protected hydroquinone and tetra(ethylene glycol) groups (1:99) was illuminated with ultraviolet light (100W Hg lamp, Nikon) filtered through a band-pass filter (365 nm) for 30 min to ensure complete deprotection of the NVOC groups to the corresponding hydroquinone.

Figure 2. Spatial and temporal control of coculture interactions. A nonfluorescent fibroblast cell line and a GFP-actin transfected cell line are used to demonstrate dynamic patterned cocultures. The microcontact-printed region contains a GFP-actin transformed cell line and the photodeprotected patterned RGD peptide gradient region with nonfluorescent fibroblasts. A) Brightfield images show both cell lines adhered (top); however, only the GFP-actin cell line is visible when visualized by fluorescence microscopy (bottom). This shows that the combined method of microcontact printing and photopatterning is effective to prepare a substrate with spatially controlled cocultures. B) Upon application of a mild reductive potential, the oxime linkage is broken and the RGD peptide ligands and adhered cells are released. This strategy selectively releases only one cell type on the surface, and allows for the spatial and temporal control of coculture interactions on surfaces. Scale bar: 100 μm.

Photopatterning of peptide ligands: UV illumination of a substrate presenting NVOC-protected hydroquinone and tetra(ethylene glycol) groups (1:99) through a photomask for 30 min removed the NVOC groups. The substrate was then oxidized electrochemically at 750 mV for 10 s to convert the hydroquinone to the quinone in PBS buffer (pH 7.4). A RGD oxyamine solution (50 mM in PBS) was added to the substrate for 1 hour to ensure complete immobilization of the peptide ligands. The substrate was then rinsed with water and dried before using for cell culture.

Cell culture: Swiss 3T3 fibroblasts were cultured in Dulbecco's Modified Eagle Medium (Gibco, Carlsbaad, CA, USA) supplemented with calf bovine serum (10%) and penicillin/streptomycin (1%). Cells were removed with a solution of trypsin (0.05%)/EDTA (0.53 mM), resuspended in serum-free culture medium (10000 cells/mL), and plated onto the SAM substrates. After 2 h, the substrates were placed in serum-containing media and maintained at 37 °C in a humidified 5% CO_2 atmosphere.

Acknowledgements

This work was supported by the Carolina Center for Cancer Nanotechnology Excellence and grants from the NIH, the Burroughs Wellcome Foundation (Interface Career Award) and the National Science Foundation (Career Award).

Keywords: cell adhesion · cell patterning · dynamic surface · electrochemistry · monolayers · photoactivation

[1] J. L. Camps, S. M. Chang, T. C. Hsu, M. R. Freeman, S. J. Hong, H. E. Zhau, A. C. von Eschenbach, L. W. Chung, *Proc. Natl. Acad. Sci. USA* **1990**, *87*, 75–79.
[2] C. S. Chen, J. Tan, J. Tien, *Annu. Rev. Biomed. Eng.* **2004**, *6*, 275–302.
[3] B. R. Clark, A. Keating, *Ann. N. Y. Acad. Sci.* **1995**, *770*, 70–78.
[4] P. F. Davies, *Lab. Invest.* **1986**, *55*, 5–24.
[5] C. vanBreemen, P. Skarsgard, I. Laher, B. McManus, X. D. Wang, *Clin. Exp. Pharmacol. Physiol.* **1997**, *24*, 989–992.
[6] R. Franco, M. I. Panayiotidis, L. D. Ochoa de la Paz, *J. Cell. Physiol.* **2008**, *216*, 14–28.
[7] C. Denef, *J. Neuroendocrinol.* **2008**, *20*, 1–70.
[8] a) B. Han, X.-H. Bai, M. Lodyga, J. Xu, B. B. Yang, S. Keshavjee, M. Post, M. Liu, *J. Biol. Chem.* **2004**, *279*, 54793–54801; b) M. K. Runyon, C. J. Kstrup, B. L. Johnson-Kerner, T. J. Van Ha, R. F. Ismagilov, *J. Am. Chem. Soc.* **2008**, *130*, 3458–3464.
[9] P. A. Janmey, D. A. Weitz, *Trends Biochem. Sci.* **2004**, *29*, 364–370.
[10] a) C. Zhao, I. Witte, G. Wittstock, *Angew. Chem.* **2006**, *118*, 5595–5597; *Angew. Chem. Int. Ed.* **2006**, *45*, 5469–5471; b) I. H. Riedel, K. Kruse, J. Howard, *Science* **2005**, *309*, 300–303; c) M. N. Yousaf, B. T. Houseman, M. Mrksich, *Proc. Natl. Acad. Sci. USA* **2001**, *98*, 5992–5996; d) M. N. Yousaf, B. T. Houseman, M. Mrksich, *Angew. Chem.* **2001**, *113*, 1127–1130; *Angew. Chem. Int. Ed.* **2001**, *40*, 1093–1096; e) C. J. Kastrup, M. K. Runyon, E. M. Lucchetta, J. M. Price, R. F. Ismagilov, *Acc. Chem. Res.* **2008**, *41*, 549–558.
[11] R. Civitelli, *Arch. Biochem. Biophys.* **2008**, *473*, 188–192.
[12] S. N. Bhatia, U. J. Balis, M. L. Yarmush, M. Toner, *FASEB J.* **1999**, *13*, 1883–1900.
[13] K. K. Hirschi, S. A. Rohovsky, P. A. D'Amore, *J. Cell Biol.* **1998**, *141*, 805–814.
[14] J. Y. Gu, X. L. Shi, Y. Zhang, Y. T. Ding, *J. Cell. Physiol.* **2009**, *219*, 100–108.
[15] G. Mbalaviele, R. Nishimura, A. Myoi, M. Niewolna, S. V. Reddy, D. Chen, J. Feng, D. Roodman, G. R. Mundy, T. Yoneda, *J. Cell Biol.* **1998**, *141*, 1467–1476.
[16] H. Zhou, W. Mak, Y. Zheng, C. R. Dunstan, M. J. Seibel, *J. Biol. Chem.* **2008**, *283*, 1936–1945.
[17] E. Aufderheide, R. Chiquet-Ehrismann, P. Ekblom, *J. Cell Biol.* **1987**, *105*, 599–608.
[18] Y. Tsuda, A. Kikuchi, M. Yamato, A. Nakao, Y. Sakurai, M. Umezu, T. Okano, *Biomaterials* **2005**, *26*, 1885–1893.
[19] M. Yamamoto, O. H. Kwon, M. Hirose, A. Kikuchi, T. Okano, *J. Biomed. Mater. Res.* **2001**, *55*, 137–140.
[20] A. Khademhosseini, L. Ferreira, J. Blumling, J. Yeh, J. M. Karp, J. Fukuda, R. Langer, *Biomaterials* **2006**, *27*, 5968–5977.
[21] S. N. Bhatia, M. L. Yarmush, M. Toner, *J. Biomed. Mater. Res.* **1997**, *34*, 189–199.
[22] A. Folch, M. Toner, *Annu. Rev. Biomed. Eng.* **2000**, *2*, 227–256.
[23] J. Fukuda, A. Khademhosseini, J. Yeh, G. Eng, J. Cheng, O. C. Farokhzad, R. Langer, *Biomaterials* **2006**, *27*, 1479–1486.
[24] H. B. Fan, H. F. Liu, S. L. Toh, J. C. H. Goh, *Biomaterials* **2008**, *29*, 1017–1027.
[25] a) S. D. Dillmore, M. N. Yousaf, M. Mrksich, *Langmuir* **2004**, *20*, 7223–7231; b) E. W. L. Chan, M. N. Yousaf, *Mol. BioSyst.* **2008**, *4*, 746–753.
[26] a) E. W. L. Chan, M. N. Yousaf, *J. Am. Chem. Soc.* **2006**, *128*, 15542–15546; b) N. P. Westcott, A. Pulsipher, B. M. Lamb, M. N. Yousaf, *Langmuir* **2008**, *24*, 9237–9240; c) W. Luo, N. P. Westcott, A. Pulsipher, M. N. Yousaf, *Langmuir* **2008**, *24*, 13096–13101; d) W. Luo, M. N. Yousaf, *Chem. Commun.* **2009**, 1237–1239; e) W. S. Yeo, M. N. Yousaf, M. Mrksich, *J. Am. Chem. Soc.* **2003**, *125*, 14994–14995.
[27] a) E. W. L. Chan, M. N. Yousaf, *ChemPhysChem* **2007**, *8*, 1469–1472; b) B. M. Lamb, N. P. Westcott, M. N. Yousaf, *ChemBioChem* **2008**, *9*, 2220–2224; c) S. Park, M. N. Yousaf, *Langmuir* **2008**, *24*, 6201–6207; d) B. M. Lamb, N. P. Westcott, M. N. Yousaf, *ChemBioChem* **2008**, *9*, 2628–2632.
[28] E. W. L. Chan, S. Park, M. N. Yousaf, *Angew. Chem.* **2008**, *120*, 6363–6367; *Angew. Chem. Int. Ed.* **2008**, *47*, 6267–6271.
[29] D. G. Barrett, M. N. Yousaf, *Angew. Chem.* **2007**, *119*, 7581–7583; *Angew. Chem. Int. Ed.* **2007**, *46*, 7437–7439.
[30] P. Harder, M. Grunze, R. Dahint, G. M. Whitesides, P. E. Laibinis, *J. Phys. Chem. B* **1998**, *102*, 426–436.
[31] M. Mrksich, C. S. Chen, Y. Xia, L. E. Dike, D. E. Ingber, G. M. Whitesides, *Proc. Natl. Acad. Sci. USA* **1996**, *93*, 10775–10778.
[32] M. D. Pierschbacher, E. Ruoslahti, *Nature* **1984**, *309*, 30–33.
[33] M. Mrksich, *Chem. Soc. Rev.* **2000**, *29*, 267–273.
[34] P. M. Mendes, *Chem. Soc. Rev.* **2008**, *37*, 2512–2529.
[35] a) D. K. Hoover, E.-j. Lee, E. W. L. Chan, M. N. Yousaf, *ChemBioChem* **2007**, *8*, 1920–1923; b) D. K. Hoover, E. W. L. Chan, M. N. Yousaf, *J. Am. Chem. Soc.* **2008**, *130*, 3280–3281.
[36] O. Collin, P. Tracqui, A. Stephanou, Y. Usson, J. Clement-Lacroix, E. Planus, *J. Cell Sci.* **2006**, *119*, 1914–1925.
[37] E. W. L. Chan, M. N. Yousaf, *Angew. Chem.* **2007**, *119*, 3955–3958; *Angew. Chem. Int. Ed.* **2007**, *46*, 3881–3884.

Received: May 3, 2009
Published online on June 23, 2009

